PHILOSOPHICAL TRANSACTIONS OF THE ROYAL SOCIETY B BIOLOGICAL SCIENCES

Constraints on models for the flagellar rotary motor

Howard C. Berg

Phil. Trans. R. Soc. Lond. B 2000 **355**, 491-501
doi: 10.1098/rstb.2000.0590

THE ROYAL SOCIETY

Constraints on models for the flagellar rotary motor

Howard C. Berg*

Departments of Molecular and Cellular Biology and Physics, Harvard University, Cambridge, MA 02138, USA, and Rowland Institute for Science, Cambridge, MA 02142, USA

Most bacteria that swim are propelled by flagellar filaments, each driven at its base by a rotary motor embedded in the cell wall and cytoplasmic membrane. A motor is about 45 nm in diameter and made up of about 20 different kinds of parts. It is assembled from the inside out. It is powered by a proton (or in some species, a sodium-ion) flux. It steps at least 400 times per revolution. At low speeds and high torques, about 1000 protons are required per revolution, speed is proportional to protonmotive force, and torque varies little with temperature or hydrogen isotope. At high speeds and low torques, torque increases with temperature and is sensitive to hydrogen isotope. At room temperature, torque varies remarkably little with speed from about −100 Hz (the present limit of measurement) to about 200 Hz, and then it declines rapidly, reaching zero at about 300 Hz. These are facts that motor models should explain. None of the existing models for the flagellar rotary motor completely do so.

Keywords: bacteria; motility; *Escherichia coli*; flagellum; rotary motor

1. STRUCTURE

About 40 gene products are involved in the construction of the flagellar rotary motor of *Escherichia coli* or *Salmonella typhimurium*, nearly half of which appear as components in the final structure (figure 1). The hook (FlgE), the hook-associated proteins (FlgK, FlgL and FliD) and the filament (FliC) are outside the cell; the MS-ring (FliF) and the P- and L-rings (FlgI and FlgH) are embedded in the cell wall; and the C-ring (FliM and FliN) is inside the cell. FliG is bound to the inner face of the MS-ring near its periphery. MotA and MotB, which are arranged in a circular array around the MS- and C-rings, span the inner (cytoplasmic) membrane.

The rings were named by DePamphilis & Adler (1971*a*), who found that the M-ring (for membrane) has affinity for inner-membrane fractions, the S-ring (for supramembranous) is seen just above the inner membrane, the P-ring (for peptidoglycan) is at the right place to span the peptidoglycan layer, and the L-ring (for lipopolysaccharide) has affinity for outer-membrane fractions (DePamphilis & Adler 1971*b*). In the earliest models for the rotary motor (Berg 1974), the M-ring was thought to rotate relative to the S-ring, which served as the stator. Later it was found that both the M- and S-rings (now called the MS-ring) comprise different domains of the same protein, FliF (Ueno *et al*. 1992, 1994). Therefore, they function as a unit. The C-ring (for cytoplasmic) was discovered much later when extracts were treated more gently, i.e. subjected to smaller extremes of pH and ionic strength (Driks & DeRosier 1990; Francis *et al*. 1994; I. M. Khan *et al*. 1992). An image reconstructed from basal bodies prepared gently and examined in frozen-hydrated preparations is included in figure 1.

FliG, FliM, and FliN also are referred to as the 'switch complex', since many mutations of *fliG*, *fliM* and *fliN* lead to defects in control of the direction of rotation (Yamaguchi *et al*. 1986*a*,*b*). Other mutations are non-motile, while the null phenotypes are non-flagellate. Functional in-frame fusions have been obtained between FliF and FliG (Francis *et al*. 1992) and between FliM and FliN (Kihara *et al*. 1996), but not between FliG and FliM (Macnab 1995). Fusions of the latter type block flagellar assembly. An electron micrographic analysis of basal-body structures found in non-motile missense mutations of *fliG*, *fliM*, and *fliN* indicates loss of the C-ring, the components of which (FliM and FliN) can be recovered in the cytoplasm (Zhao *et al*. 1995, 1996). And non-motile mutations of *fliM* and *fliN*, but not *fliG*, can be cured by overexpression (Lloyd *et al*. 1996). So attachment of the C-ring appears to be labile, as suggested by the region of low density between this structure and the rest of the basal body evident in the image reconstruction of figure 1. While it is conceivable that these structures rotate relative to one another, most workers assume that they rotate as a unit.

The stator is thought to comprise the elements MotA and MotB, proteins that are membrane embedded that do not fractionate with the rest of the hook–basal body complex (Ridgway *et al*. 1977). However, they can be visualized as circular arrays of membrane particles ('studs') in freeze-fracture preparations of the inner membrane. Studs were seen first at the poles of *Aquaspirillum serpens* in sets of 14–16 (Coulton & Murray 1978), later in *Streptococcus* in similar numbers and in *E. coli* in sets of 10–12 (Khan *et al*. 1988), and finally in

*Address for correspondence: Department of Molecular and Cellular Biology, Bio Labs Harvard, 16 Divinity Avenue, Cambridge, MA 02138, USA (hberg@biosun.harvard.edu).

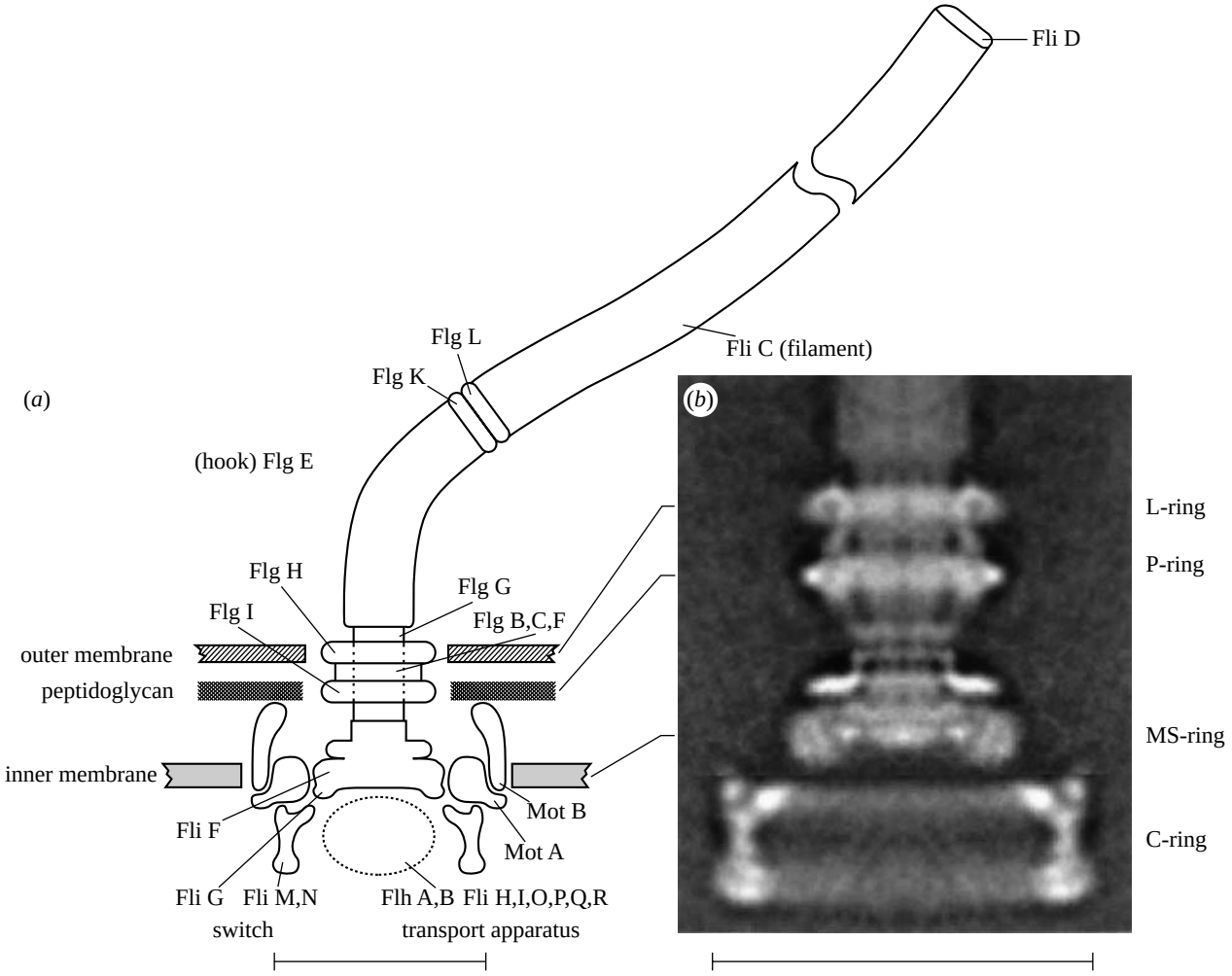

Figure 1. (*a*) A schematic diagram of the flagellar motor, drawn to scale, compared with (*b*) a rotationally averaged reconstruction of images of hook–basal bodies seen in an electron microscope. The general morphological features are C-ring, MS-ring, P-ring, L-ring, hook, hook-associated proteins (which include the distal cap) and filament. MotA, MotB and components of the transport apparatus (dashed ellipse) do not survive the procedure used to prepare samples for the electron microscope and, therefore, are not shown on the right. This picture is a rotationally averaged reconstruction of images of about 100 hook–basal bodies of *Salmonella* polyhook strain SJW880 embedded in vitreous ice (Francis *et al*. 1994). The radial densities have been projected from front to back along the line of view, so this is what would be seen if one were able to look through the spinning structure. Connections between the C-ring and the rest of the structure appear relatively tenuous. Scale bar, 45 nm. Digital print courtesy of D. J. DeRosier.

Salmonella and different species of *Bacillus* in sets of about 12 (S. Khan *et al*. 1991, 1992).

Both MotA and MotB span the cytoplasmic membrane. MotB has one membrane-spanning α-helical segment near its N-terminus, but most of the molecule is in the periplasmic space (Chun & Parkinson 1988; Stader *et al*. 1986). There is a peptidoglycan-binding domain near its C-terminus (De Mot & Vanderleyden 1994), but such binding has not been shown directly. So MotB is thought to anchor MotA to the rigid framework of the cell wall. Elements of the stator must be anchored to this framework somewhere, or torque cannot be delivered to the flagellar filament (Berg 1974). MotA has four membrane-spanning α-helical segments (Blair & Berg 1991; Dean *et al*. 1984; Zhou *et al*. 1995). The rest of the molecule (about two-thirds) is in the cytoplasm. The two Mot proteins bind to each other (Tang *et al*. 1996). Tryptophan-scanning mutagenesis suggests a model in which the transmembrane segment of MotB is bundled slantwise with the four transmembrane segments of MotA to constitute a proton channel (Sharp *et al*. 1995*a*,*b*).

Comparison of residues conserved in different bacterial species and site-directed mutagenesis have identified charged groups in the cytoplasmic domain of MotA that interact with other charged groups (primarily of opposite sign) in the C-terminal domain of FliG (Lloyd & Blair 1997; Zhou & Blair 1997; Zhou *et al*. 1998*a*). Similar studies have implicated a particular aspartate residue of MotB (Asp32) located at the cytoplasmic end of the membrane channel as a proton acceptor (Zhou *et al*. 1998*b*). And two proline residues in MotA (Pro 173, Pro 222), also located at the cytoplasmic end of this channel, have been shown to be important for function (Braun *et al*. 1999; Zhou & Blair 1997). Thus, it appears

PHILOSOPHICAL TRANSACTIONS OF THE ROYAL SOCIETY B BIOLOGICAL SCIENCES

that torque is generated as protonation, and deprotonation of Asp32 of MotB modulates the interaction of a specific charged region in the cytoplasmic domain of MotA with a complementary charged region in the C-terminal domain of FliG. Precisely how this happens is one of the key questions remaining to be answered in the study of this remarkable organelle.

2. ASSEMBLY

The motor is built from the inside out (for a short review, see Aizawa 1996). This was recognized by Suzuki *et al.* (1978), who studied mutants of *Salmonella* defective for different *fla* genes (now called *flh*, *fli* and *flg*; see Iino *et al.* 1988) and searched in pellets obtained from detergent extracts for incomplete flagellar structures. The simplest structure found was a 'rivet', comprising the MS-ring and rod. Similar results were obtained with mutants of *E. coli* (Suzuki & Komeda 1981). A more recent study identified an even simpler initial structure, the MS-ring alone, and provided many details of the morphological pathway (Kubori *et al.* 1992). FliG and the C-ring (FliM and FliN) are added to the MS-ring (FliF); see figure 1. No other proteins are required for this construction (Kubori *et al.* 1997). Then the export apparatus is assembled (FlhA, FlhB, FliH, FliI, FliO, FliP, FliQ, FliR) (see Fan *et al.* 1997; Malakooti *et al.* 1994; Ohnishi *et al.* 1997; Vogler *et al.* 1991). This apparatus is used to pass components for other axial structures through a channel at the centre of the MS-ring. But how these components are distinguished by the transport apparatus is not known. The proximal rod is added (FlgB, FlgC, FlgF) together with the longer distal rod (FlgG). FliE is needed for this assembly, but its location in the final structure is not known. Construction of the hook (FlgE) begins, but it does not proceed very far until the P- and L-rings (FlgI and FlgH) are assembled. Components for these structures are secreted into the periplasmic space by the signal-peptide-dependent (Sec) pathway (Homma *et al.* 1987; Jones *et al.* 1989). Assembly of the P-ring also requires FlgA (a chaperone?) and Dsb-catalysed formation of disulphide bonds (Dailey & Berg 1993). The L-ring is a lipoprotein (Schoenhals & Macnab 1996). The hook is assembled with the aid of a cap at its distal end (FlgD), which is then discarded (Ohnishi *et al.* 1994). Its length is determined to a precision of about 10%, but the mechanism for this control is not known (Hirano *et al.* 1994; Kutsukake *et al.* 1994). Then the hook-associated proteins (Ikeda *et al.* 1987) are added in the order HAP1 (FlgK), HAP3 (FlgL) and HAP2 (FliD). Finally, the FliC subunits (flagellin) required for growth of the filament are inserted at its distal end (Emerson *et al.* 1970; Iino 1969) under a cap (FliD). Mutants that lack FliD simply dump flagellin into the external medium (Homma *et al.* 1984). One can polymerize flagellin onto FlgL in such mutants by adding it exogenously (Kagawa *et al.* 1981, 1983) or grow filaments in the normal fashion by supplementing such mutants with endogenous FliD (Ikeda *et al.* 1993) or with FliD pre-assembled into a cap structure (Ikeda *et al.* 1996). Filament length appears to be regulated by export: filaments grow at a rate that decreases exponentially with length (Iino 1974).

3. POWER INPUT

Flagellar motors of *E. coli* and *S. typhimurium* are driven by an inward-directed proton flux, powered by a protonmotive force. Mitchell (1956, 1972) was the first to suggest that this might be so, but he had in mind iontophoretic propulsion, a process that does not require active movement of flagella. Larsen *et al.* (1974) showed that motility in *E. coli* occurs without ATP. Skulachev and his colleagues (Belyakova *et al.* 1976; Skulachev 1975) showed that motility in a Gram-negative photosynthetic bacterium *Rhodospirillum rubrum* was abolished by agents expected to collapse a transmembrane electrical potential difference and a transmembrane pH gradient, but not when these agents were added separately. Manson *et al.* (1977) obtained similar results with a motile *Streptococcus* and also were able to show that artificially imposed electrical potentials (cell interior negative) or artificially imposed pH gradients (cell interior alkaline) generate motility; protons are the only cations required for such effects. Motion in response to an artificially induced protonmotive force also was shown in *Bacillus subtilis* (Matsuura *et al.* 1977, 1979) and *R. rubrum* (Glagolev & Skulachev 1978). Anions (other than hydroxyl) have been ruled out as direct participants (Khan & Macnab 1980*a*,*b*; Ravid & Eisenbach 1984).

The protonmotive force, Δp, is the work per unit charge that a proton can do in crossing the cytoplasmic membrane. In general, it comprises two terms, one due to the transmembrane electrical potential difference, $\Delta\psi$, and the other to the transmembrane pH difference ($-2.3\,kTe^{-1}$) ΔpH, where k is Boltzmann's constant, T the absolute temperature, and e the proton charge. At 24 °C, $2.3\,kTe^{-1} = 59$ mV. By convention, $\Delta\psi$ is the internal potential less the external potential, and ΔpH is the internal pH less the external pH. *E. coli* maintains its internal pH in the range 7.6–7.8. For cells grown at pH 7, $\Delta p \approx -170$ mV, $\Delta\psi \approx -120$ mV, and $-59\Delta\text{pH} \approx -50$ mV. For cells grown at pH 7.6–7.8, $\Delta p \approx \Delta\psi \approx -140$ mV. For a general discussion of chemiosmotic energy coupling, see Harold & Maloney (1996). For a review of methods for measuring Δp, see Kashket (1985).

The only measurement of proton flux that has been made is with motors of the motile *Streptococcus* sp. strain V4051 (Van der Drift *et al.* 1975), a peritrichously flagellated, primarily fermentative, Gram-positive organism that lacks an endogenous energy reserve and is sensitive to ionophores and uncouplers. Unlike *E. coli*, this organism can be starved and artificially energized, either with a potassium diffusion potential (by treating cells with valinomycin and shifting them to a medium with a lower concentration of potassium ion) or with a pH gradient (by shifting cells to a medium of lower pH); see Manson *et al.* (1977, 1980). If this is done with a medium of low buffering capacity, one can follow proton uptake by the increase in external pH. The frequency of rotation of filaments in flagellar bundles can be determined by monitoring the swimming speed—the experiments were done with a smooth-swimming mutant—given the ratio of swimming speed to bundle frequency determined separately by video taping cells under phase-contrast microscopy and measuring their vibration frequencies by power spectral analysis; see Lowe *et al.* (1987). Finally, the

data can be normalized to single motors by counting the number of cells and the number of flagellar filaments per cell. The total proton flux into the cell is much larger than the flux through its flagellar motors. However, the two can be distinguished by suddenly stopping the motors by adding an anti-filament antibody—this cross-links adjacent filaments in the flagellar bundles (see Berg & Anderson 1973)—and measuring the change in flux. This change is directly proportional to the initial swimming speed, as would be expected if a fixed number of protons carry a motor through each revolution. This number is about 1200 (Meister *et al*. 1987).

The flux through the flagellar motor is divided into as many as eight distinct proton channels, comprising one or more copies of the proteins MotA and MotB (figure 1). Restoration of motility in paralysed *motB* cells was studied by Block & Berg (1984), who tethered such-cells to a glass surface by a single flagellum (Silverman & Simon 1974) and expressed the wild-type gene from a plasmid under control of the *lac* promoter. This work was extended to MotA in a more carefully controlled study by Blair & Berg (1988). Resurrection occurs in a number of equally spaced steps, indicating that each additional torque-generating element adds the same increment of torque. The main argument for a complement of eight such torque-generating units is that resurrections of this kind have produced eight equally spaced levels more than once, but never nine. As noted above, the number of studs seen in freeze-fracture experiments ranges from about 10 to 16. In particular, the number seen for *E. coli* is 10–12 (Khan *et al*. 1988). Blair & Berg (1988), wondering whether this might represent an incomplete set, produced MotA and MotB at a slight excess of wild-type levels and found that the torque increased by about 20%. They also found that the torque for wild-type motors was only about five times that for a one-generator motor, whereas following complete resurrection, this factor was about eight. So it is possible that the full complement of torque generators is eight and the full complement of studs is 16.

It is likely that the passage of each proton (or perhaps each proton pair) moves a torque generator (a MotA, MotB complex) one step (one binding site) along the periphery of the rotor, suddenly stretching the components that link that generator to the rigid framework of the cell wall. As this linkage relaxes, a tethered cell should rotate by a fixed increment. In other words, the motor should behave like a stepping motor. Since proton passage is likely to occur at random times, the steps will occur with exponentially distributed waiting times. We have been looking for such steps since 1976 (Berg 1976), but without success. The main reason, advanced then, is that the torque applied to the structure linking the rotor to the tethering surface (a series of elastic elements, comprising the rod, hook and filament) causes that structure to twist. When less torque is applied, these elements untwist, carrying the cell body forward. Therefore, discontinuities in the relative motion of rotor and stator are smoothed out. To succeed, one probably needs to work at reduced torque, e.g. with a one-generator motor driving a small viscous load, perhaps just a hook. Such an object is expected to spin quite rapidly, so the technical problems are formidable.

One route around this difficulty is to examine variations in rotation period. If k steps occur at random each revolution, then the ratio of the standard deviation to the mean should be $1/\sqrt{k}$ (see Cox & Lewis 1966, p. 24; Samuel & Berg 1995, appendix). An early analysis of this kind led to an estimate of about 400 (Berg *et al*. 1982), which has been borne out by more recent work (Samuel & Berg 1995). The more recent analysis also showed that a tethered cell is restrained: it is not free to execute rotational Brownian motion. Thus, the rotor and stator are interconnected most of the time.

This stochastic analysis was repeated with tethered cells undergoing resurrection, and the number of steps per revolution was found to increase linearly with level number, increasing by about 50 steps per level (Samuel & Berg 1996). Thus, each force generator steps independently of all the others (consistent with the fact that each adds the same increment of torque), and each remains connected to the rotor most of the time (consistent with the absence of free rotational Brownian movement). The latter conclusion resolves the following conundrum. If torque generators interact with a fixed number of binding sites on the rotor, say 50, then why is the number of steps per revolution not just 50? If n torque generators are attached to the rotor and one steps, suddenly stretching its linkage to the rigid framework of the cell wall, then when that linkage relaxes and moves the rotor, it also must stretch the linkages of the $n-1$ torque generators that have not stepped. If $n=2$, the net movement of the rotor is half of what it would be at $n=1$, so the apparent step number is 100 per revolution. If $n=8$, the apparent step number is 400 per revolution. If, on the other hand, each torque generator remained detached most of the time (for most of its duty cycle), then the apparent step number would remain 50.

If steps occur at random, then the numbers 50, 100 ... 400 all are lower bounds. The smoother the rotation, the larger the estimate of the number of steps per revolution. Therefore, any noise in the system that adds to variation in rotation period reduces that estimate. If steps do not occur at random, i.e. if steps are clocked or successive steps are not independent of one another, then similar statistics could be generated with fewer steps; see Svoboda *et al*. (1994).

Coarser fluctuations, probably associated with variations in the number of active torque-generating units, have been studied by Kara-Ivanov *et al*. (1995).

How does the proton flux vary with protonmotive force? Or equivalently, given that a fixed number of protons carries the motor through each revolution, how does the rotation speed vary with protonmotive force? In the earliest work with tethered cells, chemical methods were used to generate potassium diffusion potentials or pH gradients (Conley & Berg 1984; Khan & Berg 1983; Khan *et al*. 1985; Manson *et al*. 1980; Meister & Berg 1987). This work, done with *Streptococcus*, showed that speed is proportional to protonmotive force up to at least -80 mV and that potential shifts or pH shifts are energetically equivalent. A composite relationship for *Streptococcus* approximately linear up to -190 mV was obtained by including data from glycolysing cells (Khan *et al*. 1990). Large voltages have been applied to cells of *S. typhimurium* held by micropipettes, but not under

conditions in which the membrane potential was known (Kami-ike *et al*. 1991). More controlled energization was achieved by pulling filamentous cells of *E. coli* roughly halfway into micropipettes, permeabilizing the cytoplasmic membrane of that part of the cell inside the pipette with gramicidin S, and then watching an inert marker attached to the hook (polyhook) of a flagellar motor on that part of the cell outside the pipette (Fung & Berg 1995). Application of an electrical potential between the external medium and inside of the pipette (the latter negative) caused the marker to spin, and its rotation speed proved to be directly proportional to Δp.

Motors appear to slow down at extremes of pH (usually external pH) below 6 or above 9. This is true both for tethered cells (Khan *et al*. 1990; Meister & Berg 1987) and for swimming cells (Khan *et al*. 1990; Khan & Macnab 1980*a*,*b*; Shioi *et al*. 1980). However, swimming cells show thresholds below which cells do not swim ($\Delta p \approx -30$ mV) and above which speed saturates ($\Delta p \approx -100$ mV), neither of which is evident with tethered cells. These thresholds might be due to problems with bundle formation and changes in filament shape, respectively. More work needs to be done with single motors operating at high speed.

It is important to recognize that some bacteria (marine bacteria or bacteria that live at high pH) drive their flagellar motors with sodium ions rather than with protons; for early reviews, see Imae (1991) and Imae & Atsumi (1989). Thus, flagellar motors are ion driven, not just proton driven. When flagella are driven with a large sodium gradient, their rotation speeds can be remarkably high, up to 1700 Hz (Magariyama *et al*. 1994; Muramoto *et al*. 1995). And rotation can be blocked with specific inhibitors of sodium transport, such as amiloride (Sugiyama *et al*. 1988) or phenamil (Atsumi *et al*. 1990). This has made it possible to screen for sodium-channel mutants (Kojima *et al*. 1997, 1999).

The power input to the motor, the rate at which protons can do work, is proton flux times proton charge times Δp. If we use as a benchmark a tethered *E. coli* spinning at 10 Hz at pH 7 ($\Delta p \approx -170$ mV) and assume a proton flux of 1200 per revolution—this is the least well known of all of these quantities—then the power input is $(1.2 \times 10^4\,\mathrm{s}^{-1})\ (e)\ (0.17\ \mathrm{V}) \approx 2.0 \times 10^3\,\mathrm{eV\,s}^{-1}$ (electron volts per second, with $1\,\mathrm{eV} = 1.6 \times 10^{-12}\,\mathrm{erg} = 1.6 \times 10^{-19}\,\mathrm{J}$).

4. POWER OUTPUT

The torque, $\mathcal{N}$, required to rotate an object of fixed shape in a viscous medium is its rotational frictional drag coefficient, f, multiplied by its angular velocity, Ω (2π times its rotation speed, in Hz). In a torque versus speed plot, this function is a straight line passing through the origin, with slope f. Two such lines are shown in figure 2 (thin lines), one for the cell body of an average-sized wild-type cell, the other for a smaller minicell. Here, we assume that the medium is Newtonian, i.e. that the frictional drag coefficient does not depend on Ω, a condition satisfied in a dilute aqueous medium that does not contain long unbranched molecules, such as methylcellulose or polyvinylpyrrolidone (Berg & Turner 1979). For such a medium, f is a geometrical factor multiplied by the bulk viscosity, η, where η is independent of Ω (independent of the rate of shear). For an isolated sphere of radius a, spinning about an axis through its centre, this geometrical factor is $8\pi a^3$. For compact globular objects, the actual shape is not very critical; however, accurate values can be computed (Garcia de la Torre & Bloomfield 1981). The distance from the tethering surface does not really matter, either, provided that the gap between the cell and the surface is at least 0.2 radii (Berg 1976; Jeffery 1915). So, the torque required to spin the cell body of *E. coli* (approximated as a sphere of radius 1 μm) at 10 Hz in water is approximately $8\pi a^3 \eta \Omega$, which in cgs units is $8\pi(10^{-12})\ (10^{-2})\ 2\pi(10) = 1.6 \times 10^{-11}$ dyn-cm. The power required to sustain this rotation is $\mathcal{N}\Omega$, or $1.0 \times 10^{-9}\,\mathrm{erg\,s}^{-1} \approx 0.6 \times 10^3\,\mathrm{eVs}^{-1}$ (Berg 1974). So, by this crude estimate, the motor is about 30% efficient: compare the figure for power input, $2 \times 10^3\,\mathrm{eVs}^{-1}$, given at the end of § 3. Crude estimates ranging from 50 to 90% have been made from more accurate computations with data obtained from *Streptococcus* (Meister *et al*. 1987). Within the uncertainty of the measurements, the efficiency could be 1.

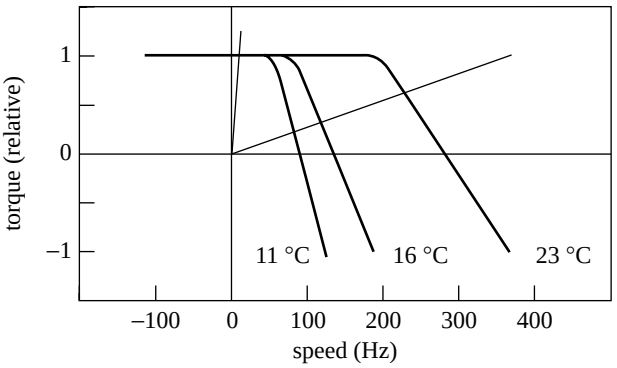

Figure 2. The torque–speed curve for the flagellar motor of *E. coli* shown at three temperatures (thick lines), together with two load lines (thin lines), one for an object the size of the cell body of wild-type *E. coli* (effective radius about 1 μm, left), the other for a minicell (effective radius about 0.3 μm, right). Adapted from Berg & Turner (1993, fig. 16).

We would like to know how the torque generated by the flagellar motor varies with speed. At low speeds, it is approximately constant, because the speed of tethered cells is inversely proportional to the viscosity of the external medium, which can be varied by addition of Ficoll™ (Amersham Pharmacia Biotech, Uppsala, Sweden) (Berg & Turner 1979; Manson *et al*. 1980). At the higher speeds encountered with swimming cells, torque declines with speed (Lowe *et al*. 1987). Measurements have been made with tethered cells of *E. coli* over a wide range of speeds, including speeds in which the motor is driven backwards, with the results shown in figure 2 (thick lines). The torque exerted by the motor of *E. coli* is approximately constant, all the way from negative speeds of at least −100 Hz to positive speeds of nearly 200 Hz (at 23 °C). At higher speeds it declines approximately linearly, crossing the zero-torque line at about 300 Hz. At lower temperatures, the region of transition from constant torque to declining torque shifts to lower speeds, and the region of decline steepens (Berg & Turner 1993). Data obtained at different temperatures can be mapped onto one another with scaling of the speed axis.

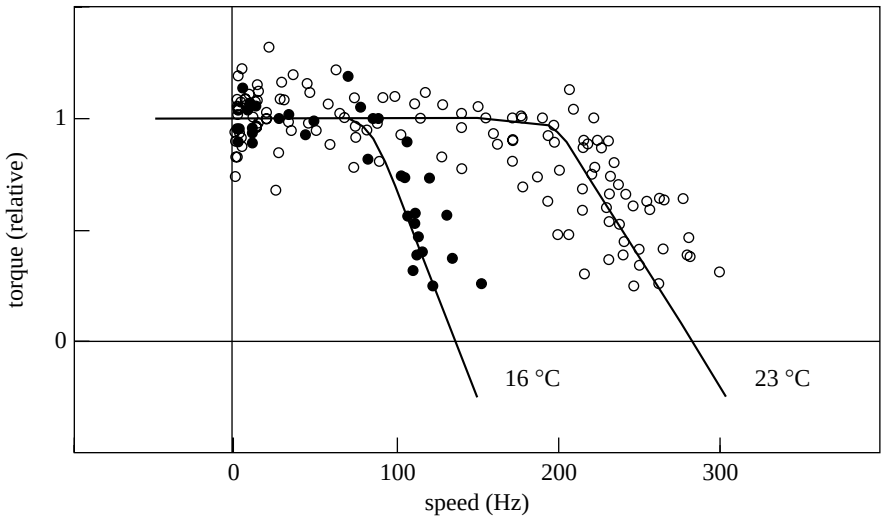

Figure 3. The torque–speed curve for the flagellar motor of *E. coli* shown at two temperatures. Data summarized in figure 2 (solid lines) are compared with data obtained at 16 °C (solid symbols, 11 cells) or 23 °C (open symbols, 30 cells) by increasing the steepness of the load line of small latex beads spinning on a flagellar-filament stub by addition of Ficoll™. Viscosities and speeds were recorded, and the quantity viscosity × speed was plotted as a function of speed, with normalization to 1 at low speed.

Before more is said about how the torque–speed curve is measured, note that a motor obeying such a curve will spin at the speed at which the torque–speed curve intersects the load line for the object being spun, i.e. at the speed at which the torque generated by the motor is balanced by the torque due to external viscous drag. At 23 °C and for the load line shown at the left in figure 2, this speed is 10 Hz; for the load line shown at the right, it is about 220 Hz. For a very shallow load line, e.g. for that of a free hook, the speed would be close to the zero-torque speed, about 290 Hz. A motor free-running in this way always operates in the upper right-hand quadrant of figure 2. It cannot drive itself backwards, although, it can redefine what is meant by forwards by switching from counterclockwise (CCW) to clockwise (CW) or back again. Nor can it spin faster than possible at zero load. To probe the upper left- or lower right-hand quadrants of figure 2, one needs to subject the motor to torque applied externally.

In our early work, we had thought that there was an abrupt barrier to backwards rotation (Berg & Turner 1993), but this proved to be an artefact of the method employed for generating the externally applied torque (Berry & Berg 1997). Cells were tethered and exposed to a high-frequency rotating electric field (Washizu *et al.* 1993), at 2.25 MHz in our experiments (Berg & Turner 1993). As explained in the latter reference, the external electric field polarizes the cell. The dipole field due to the polarization rotates at the same rate and in the same direction as the applied electric field. However, due to the finite time required for redistribution of charges, the polarization vector leads or lags the electric-field vector. The externally applied torque is the cross-product of these vectors. The applied torque varies as the square of the magnitude of the electric field and changes sign with changes in the direction of rotation of that field. Therefore, it is possible to spin a tethered cell either forwards or backwards. Speeds of several hundred Hertz are readily attainable (Berg & Turner 1993). For reasons that we do not understand, the motor of a cell driven backwards (CW if it is trying to spin CCW, or CCW if it is trying to spin CW) often breaks catastrophically: motor torque suddenly drops to zero, the cell appears free to execute rotational Brownian motion, and the motor fails to recover. Our best guess is that the C-ring is sheared off of the bottom of the rotor (figure 1), disengaging all torque-generating units but leaving the bearings intact. If one were to break the rod, the cell would simply come off the tethering surface. We know this, because there are mutants in the gene for the MS-ring that weaken the rod MS-ring attachment, allowing rod, hook and filament to pull out of the cell (Okino *et al.* 1989). In any event, once the motor has broken, one can compare the speed at which the cell body turns at a given value of externally applied torque with the speed at which it turned at the same value of externally applied torque before the break occurred. The difference is proportional to the torque generated by the motor at the speed at which it turned when it was intact. The data shown by the thick lines in figure 2 were gathered in this way.

A problem arises when the electric-field vector follows an elliptical rather than a circular path, e.g. when the sets of electrodes used to generate the rotating field are not equally spaced. In that event, the externally applied torque depends on cell angle. When one tries to drive the motor backwards by running the applied electric field in the appropriate direction and increasing its magnitude, the cell body slows down until a point is reached at which the externally applied torque is larger than the motor torque at some angles but smaller than the motor torque at other angles. Then the cell body stops at an intermediate angle, i.e. at an angle at which the two torques balance. It remains stopped until the applied torque is larger than motor torque at all angles (see Berry & Berg 1999, fig. 2). Since the model that we were trying to test predicts a barrier to backwards rotation (Meister *et al.* 1989), we erred by interpreting this stoppage as such a barrier. The matter has been resolved by using optical tweezers to drive cells backwards (Berry & Berg 1997) and by reanalysing some of the electrorotation data (Berry & Berg 1996) as a function of cell angle (Berry & Berg 1999). The results for backwards rotation are those shown in figure 2, namely, a torque–speed curve that is nearly flat all the way back to −100 Hz. Our analysis does not rule out the possibility that motor torque declines linearly with speed over the region −100 to +100 Hz (at 23 °C), but the data are consistent with zero slope. The possibility of finite (presumably negative) slope

PHILOSOPHICAL TRANSACTIONS OF THE ROYAL SOCIETY B BIOLOGICAL SCIENCES

is being checked in experiments (in progress) in which the steepness of the load line for a small latex bead spinning on a flagellar-filament stub is increased by addition of Ficoll™. The results obtained thus far, shown in figure 3, are completely consistent with those of figure 2. The torque is approximately constant up to relatively high speed (at 23 °C, falling from 1 to about 0.9 at the knee), and then it drops nearly linearly to the zero-torque speed, with the position of the boundary between these two regimes strongly dependent on temperature (see Chen & Berg 2000).

When the motor spins slowly, it appears to operate near thermodynamic equilibrium, where rates of displacement of internal mechanical components or translocation of protons are not limiting. This was shown directly by energizing tethered cells of *Streptococcus* with a potassium diffusion potential and varying the temperature from 4 to 38 °C or replacing H_2O in the external medium with D_2O. The resulting changes in torque were at most a few per cent (Khan & Berg 1983). However, when the motor spins rapidly, this is not the case, as evident in figure 2 and 3, where torque drops at lower temperatures. In this high-speed regime, shifts from H_2O to D_2O also reduce torque (Blair & Berg 1990; Meister *et al*. 1987).

Note that the power output, $N\Omega$, increases linearly with speed up to the boundary between the low-speed and high-speed regimes and then declines (figure 2). If, as indicated earlier, a fixed number of protons carries the motor through each revolution, then power input also increases linearly with speed. Therefore, the efficiency is approximately constant up to the boundary between the low- and high-speed regimes, and then it declines. There is no discontinuity in torque as one crosses the zero-speed axis (Berry & Berg 1997). As the motor turns backwards, it must pump protons, just as the F_0–ATPase pumps protons when driven backwards by F_1.

Why is the low-speed regime so broad, and why is the boundary between the low- and high-speed regimes so narrow? And why is the position of that boundary so sensitive to temperature?

5. MODELS

The fundamental question is how the flagellar motor generates torque, namely, how inward motion of one or more ions through a torque-generating unit causes it to advance circumferentially along the periphery of the rotor. Once that is understood, the nature of the conformational change required for switching, namely, how the direction of advance is distinguished from that of retreat, is likely to be self-evident.

Criteria for success in modelling should be based on the behaviour of individual motors, not groups of motors, as reflected in the way in which peritrichously flagellated bacteria swim. Mechanical interactions between different flagellar filaments are not well understood. Even if rotation rates of flagellar bundles are known (Lowe *et al*. 1987), it is not obvious how motor torque scales with filament number.

Moving parts of the motor are submicroscopic and immersed in a viscous medium (water or lipid), so everything is overdampened; the Reynolds number is very small (Berg 1996; Ludwig 1930; Purcell 1977; Taylor 1952). There is no inertia in the problem; no flywheel. If, for example, the operator of the motor driving a tethered cell of *E. coli* at 10 Hz were to put in the clutch, the cell body would coast no more than a millionth of a revolution (Berg 1974). So, if there is a stage in the rotational cycle in which the torque changes sign, the motor will stop. Predicting net torque after averaging over a complete cycle is not sufficient. And mechanisms in which energy is stored in vibrational modes simply will not work. However, one can use energy available from an electrochemical potential to stretch a spring and then use that spring to apply a steady force.

The force required is modest. Estimates of the torque generated by a wild-type motor range from about 2700 to 4600 pN nm (piconewton nanometres), 2700 estimated from the viscous drag on tethered cells of *Streptococcus* (Lowe *et al*. 1987), 4600 from the force exerted by tethered cells of *E. coli* on latex beads held in an optical trap (Berry & Berg 1997). If we take an approximate figure of 4000 and assume that force-generating units act at the periphery of the rotor at a radius of about 20 nm, then 200 pN are applied. If there are eight independent force-generating units (Blair & Berg 1988), then each contributes 25 pN. This force is substantial compared with that generated by other motor molecules; however, it is not large on an absolute scale. It is a force equal in magnitude to that between two electrons 4.8 Å apart in a medium of dielectric constant 40 (midway between water, 80, and lipid, about 2). So, almost any kind of chemistry will do.

Motion of the torque-generating units relative to the periphery of the rotor is driven by a proton (or sodium-ion) flux. Only one experiment has attempted to measure this flux (Meister *et al*. 1987), and flux and speed were found to be linearly related. Unless protons flow through the motor when it is stalled, this implies that a fixed number of protons carries the motor through each revolution. The running torque at low speeds is close to the stall torque (figure 2). If the motor is stalled and no protons flow, no free energy is dissipated; therefore, the stalled motor is at thermodynamic equilibrium. For slow rotation near stall, the motor must operate reversibly at unit efficiency, with the free energy lost by protons traversing the motor equal to the mechanical work that it performs. This implies that the torque near stall should be proportional to the protonmotive force over its full physiological range, as observed (Fung & Berg 1995). So the evidence is consistent with a model in which the motor is tightly coupled.

An important question is whether the ion that moves down the electrochemical gradient is directly involved in generating torque, i.e. participates in a power stroke in which dissipation of energy available from the electrochemical gradient and rotational work occur synchronously, or whether the ion is indirectly involved in generating torque, e.g. by enabling a ratchet which is powered thermally. In the power stroke case, protons can be driven out of the cell by backwards rotation and steep barriers are not expected. In addition, if the rate-limiting step is strongly torque dependent, then the torque–speed curve (as plotted in figure 2) can have a relatively flat plateau, because small changes in torque can generate large changes in speed (Berry & Berg 1999). In the

ratchet case, with tight coupling, the likelihood of transit of ions against the electrochemical gradient is small, so the system must wait, even when large backwards torques are applied, and barriers to backwards rotation are expected. Also, the torque–speed curves are relatively steep (Berry & Berg 1999). So the torque–speed curves of figure 2 favour a power stroke mechanism. For kinetic analyses of power stroke or ratchet mechanisms equivalent to those in Berry & Berg (1999), see Iwazawa *et al*. (1993) and Khan *et al*. (1990), respectively.

It is of interest to compare the force estimate of 25 pN with the force one would expect for tight coupling. The work that a proton can do in crossing the membrane is $e\Delta p$, with $\Delta p \approx -170$ mV; see § 3. At unit efficiency, this work is equal to the work that the force generator can do, Fd, where F is the force and d the displacement per proton used. Assuming 50 steps per revolution (Samuel & Berg 1996) and a rotor radius of 20 nm, $d \approx 2.5$ nm. So $F \approx 11$ pN. If two protons are required per elementary step or if the steps are half as long, then $F \approx 22$ pN. For loose coupling, the efficiency is less than one, and the force generated is smaller.

Tightly coupled models can be distinguished from one another only by their behaviour at high speeds, far from the point of thermodynamic equilibrium. A seminal test for any such model is the torque–speed curve of figure 2. The thermal-ratchet model that we proposed (Berg & Khan 1983; Meister *et al*. 1989), which with improvements has been applied successfully to F_0 (Elston & Oster 1997), fails this test. At negative speeds, it predicts barriers to rotation, and at positive speeds, it predicts a torque that falls steadily toward the zero-torque speed. It does not predict a constant-torque plateau or an abrupt transition from a low- to a high-speed regime; see Meister *et al*. (1989, fig. 7).

Finally, a successful model must be consistent with the general structural features outlined in figure 1, where the filament, hook, rod, MS-ring and FliG rotate relative to the rigid framework of the cell, defined by the peptidoglycan layer, and the Mot proteins do not. As argued earlier, FliM and FliN are probably part of the rotor; however, the evidence for this is not conclusive. Also, there appear to be essential electrostatic interactions between specific residues in the cytoplasmic domain of MotA and the C-terminal domain of Fli-C (Zhou *et al*. 1998*a*). Here, charge complementarity is more important than surface complementarity, i.e., long-range interactions appear to be more important than tight binding. Since some models for torque generation require transfer of protons from the stator to the rotor, it was expected that acidic residues on FliG might be more important than basic residues. However, replacement of the acidic residues deemed important for torque generation with alanine still allowed some rotation, while reversing their charge had a more severe effect (Lloyd & Blair 1997). An extension of this study failed to identify any conserved basic residues critical for rotation in MotA, MotB, FliG, FliM or FliN and only one conserved acidic residue critical for rotation, Asp32 of MotB (Zhou *et al*. 1998*b*). Other alternatives were considered and either ruled out or deemed unlikely. Therefore, the only strong candidate for a residue that functions directly in proton conduction is Asp32 of MotB.

For concise surveys of existing models, see Berg & Turner (1993), Caplan & Kara-Ivanov (1993) and Läuger & Kleutsch (1990). For more recent work, see Elston & Oster (1997).

Given the work of Blair and colleagues, I favour a cross-bridge mechanism of the kind envisaged by Läuger (model II of Läuger (1988)). In this scheme, proton transport drives a cyclic sequence in which (i) a proton binds to an outward-facing binding site (presumably, Asp32 of MotB), (ii) the protonmotive force drives a conformational change, a power stroke (Berry & Berg 1999) that moves the rotor forward (or stretches a spring that moves it forward) and transforms the binding site to an inward-facing site, and (iii) proton dissociation triggers detachment of the cross-bridge from the rotor, its relaxation to the original shape, and reattachment to an adjacent site. If step (iii) is relatively fast, the cross-bridge will remain attached to the rotor most of the time. However, it is difficult to formulate such a model in detail without more structural information. Obtaining such information is the most pressing task of the future.

I thank Xiaobing Chen for the new torque-speed data, Karen Fahrner, Lloyd Schoenbach and Linda Turner for help with the figures and Richard Berry for comments on the manuscript. This paper is adapted from a longer review scheduled to appear in a volume of *The Enzymes* on molecular motors. Work done in the author's laboratory has been supported by the US National Institutes of Health, the US National Science Foundation, and the Rowland Institute for Science.

REFERENCES

Aizawa, S.-I. 1996 Flagellar assembly in *Salmonella typhimurium*. *Mol. Microbiol.* **19**, 1–5.

Atsumi, T., Sugiyama, S., Cragoe Jr, E. J. & Imae, Y. 1990 Specific inhibition of the Na^+-driven flagellar motors of alkalophilic *Bacillus* strains by the amiloride analog phenamil. *J. Bacteriol.* **172**, 1634–1639.

Belyakova, T. N., Glagolev, A. N. & Skulachev, V. P. 1976 Electrochemical gradient of H^+ ions as a direct source of energy during bacterial locomotion. *Biochemistry* **41**, 1206–1210.

Berg, H. C. 1974 Dynamic properties of bacterial flagellar motors. *Nature* **249**, 77–79.

Berg, H. C. 1976 Does the flagellar rotary motor step? In *Cell motility, Cold Spring Harbor conferences on cell proliferation*, vol. 3 (ed. R. Goldman, T. Pollard & J. Rosenbaum), pp. 47–56. Cold Spring Harbor, NY: Cold Spring Harbor Laboratory.

Berg, H. C. 1996 Symmetries in bacterial motility. *Proc. Natl Acad. Sci. USA* **93**, 14 225–14 228.

Berg, H. C. & Anderson, R. A. 1973 Bacteria swim by rotating their flagellar filaments. *Nature* **245**, 380–382.

Berg, H. C. & Khan, S. 1983 A model for the flagellar rotary motor. In *Mobility and recognition in cell biology* (ed. H. Sund & C. Veeger), pp. 485–497. Berlin: deGruyter.

Berg, H. C. & Turner, L. 1979 Movement of microorganisms in viscous environments. *Nature* **278**, 349–351.

Berg, H. C. & Turner, L. 1993 Torque generated by the flagellar motor of *Escherichia coli*. *Biophys. J.* **65**, 2201–2216.

Berg, H. C., Manson, M. D. & Conley, M. P. 1982 Dynamics and energetics of flagellar rotation in bacteria. *Symp. Soc. Exp. Biol.* **35**, 1–31.

Berry, R. M. & Berg, H. C. 1996 Torque generated by the bacterial flagellar motor close to stall. *Biophys. J.* **71**, 3501–3510.

Berry, R. M. & Berg, H. C. 1997 Absence of a barrier to backwards rotation of the bacterial flagellar motor demonstrated with optical tweezers. *Proc. Natl Acad. Sci. USA* **94**, 14 433–14 437.

Berry, R. M. & Berg, H. C. 1999 Torque generated by the flagellar motor of *Escherichia coli* while driven backwards. *Biophys. J.* **76**, 580–587.

Blair, D. F. & Berg, H. C. 1988 Restoration of torque in defective flagellar motors. *Science* **242**, 1678–1681.

Blair, D. F. & Berg, H. C. 1990 The MotA protein of *Escherichia coli* is a proton-conducting component of the flagellar motor. *Cell* **60**, 439–449.

Blair, D. F. & Berg, H. C. 1991 Mutants in the MotA protein of *Escherichia coli* reveal domains critical for proton conduction. *J. Mol. Biol.* **221**, 1433–1442.

Block, S. M. & Berg, H. C. 1984 Successive incorporation of force-generating units in the bacterial rotary motor. *Nature* **309**, 470–472.

Braun, T. F., Poulson, S., Gully, J. B., Empey, J. C., Van Way, S., Putnam, A. & Blair, D. F. 1999 Function of proline residues of MotA in torque generation by the flagellar motor of *Escherichia coli*. *J. Bacteriol.* **181**, 3542–3551.

Caplan, S. R. & Kara-Ivanov, M. 1993 The bacterial flagellar motor. *Int. Rev. Cytol.* **147**, 97–164.

Chen, X. & Berg, H. C. 2000 Torque–speed relationships of the flagellar rotary motor of *Escherichia coli*. *Biophys. J.* **78**, 1036–1041.

Chun, S. Y. & Parkinson, J. S. 1988 Bacterial motility: membrane topology of the *Escherichia coli* MotB protein. *Science* **239**, 276–278.

Conley, M. P. & Berg, H. C. 1984 Chemical modification of *Streptococcus* flagellar motors. *J. Bacteriol.* **158**, 832–843.

Coulton, J. W. & Murray, R. G. E. 1978 Cell envelope associations of *Aquaspirillum serpens* flagella. *J. Bacteriol.* **136**, 1047–1049.

Cox, D. R. & Lewis, P. A. W. 1966 *The statistical analysis of series of events*. London: Methuen.

Dailey, F. E. & Berg, H. C. 1993 Mutants in disulfide bond formation that disrupt flagellar assembly. *Proc. Natl Acad. Sci. USA* **90**, 1043–1047.

Dean, G. E., Macnab, R. M., Stader, J., Matsumura, P. & Burke, C. 1984 Gene sequence and predicted amino acid sequence of the MotA protein, a membrane-associated protein required for flagellar rotation in *Escherichia coli*. *J. Bacteriol.* **159**, 991–999.

De Mot, R. & Vanderleyden, J. 1994 The C-terminal sequence conservation between OmpA-related outer membrane proteins and MotB suggests a common function in both Gram-positive and Gram-negative bacteria, possibly in the interaction of these domains with peptidoglycan. *Mol. Microbiol.* **12**, 333–334.

DePamphilis, M. L. & Adler, J. 1971*a* Fine structure and isolation of the hook–basal body complex of flagella from *Escherichia coli* and *Bacillus subtilis*. *J. Bacteriol.* **105**, 384–395.

DePamphilis, M. L. & Adler, J. 1971*b* Attachment of flagellar basal bodies to the cell envelope: specific attachment to the outer, lipopolysaccharide membrane and the cytoplasmic membrane. *J. Bacteriol.* **105**, 396–407.

Driks, A. & DeRosier, D. J. 1990 Additional structures associated with bacterial flagellar basal body. *J. Mol. Biol.* **211**, 669–672.

Elston, T. C. & Oster, G. 1997 Protein turbines. I. The bacterial flagellar motor. *Biophys. J.* **73**, 703–721.

Emerson, S. U., Tokuyasu, K. & Simon, M. I. 1970 Bacterial flagella: polarity of elongation. *Science* **169**, 190–192.

Fan, F., Ohnishi, K., Francis, N. R. & Macnab, R. M. 1997 The FliP and FliR proteins of *Salmonella typhimurium*, putative components of the type III flagellar export apparatus, are located in the flagellar basal body. *Mol. Microbiol.* **26**, 1035–1046.

Francis, N. R., Irikura, V. M., Yamaguchi, S., DeRosier, D. J. & Macnab, R. M. 1992 Localization of the *Salmonella typhimurium* flagellar switch protein FliG to the cytoplasmic M-ring face of the basal body. *Proc. Natl Acad. Sci. USA* **89**, 6304–6308.

Francis, N. R., Sosinsky, G. E., Thomas, D. & DeRosier, D. J. 1994 Isolation, characterization and structure of bacterial flagellar motors containing the switch complex. *J. Mol. Biol.* **235**, 1261–1270.

Fung, D. C. & Berg, H. C. 1995 Powering the flagellar motor of *Escherichia coli* with an external voltage source. *Nature* **375**, 809–812.

Garcia de la Torre, J. & Bloomfield, V. A. 1981 Hydrodynamic properties of complex, rigid, biological macromolecules: theory and applications. *Q. Rev. Biophys.* **14**, 81–139.

Glagolev, A. N. & Skulachev, V. P. 1978 The proton pump is a molecular engine of motile bacteria. *Nature* **272**, 280–282.

Harold, F. M. & Maloney, P. C. 1996 Energy transduction by ion currents. In Escherichia coli *and* Salmonella*: cellular and molecular biology*, vol. 1 (ed. F. C. Neidhardt, R. Curtiss, J. L. Ingraham, E. C. C. Lin, K. B. Low, B. Magasanik, W. S. Reznikoff, M. Riley, M. Schaechter & H. E. Umbarger), pp. 283–306. Washington, DC: American Society for Microbiology.

Hirano, T., Yamaguchi, S., Oosawa, K. & Aizawa, S.-I. 1994 Roles of FliK and FlhB in determination of flagellar hook length in *Salmonella typhimurium*. *J. Bacteriol.* **176**, 5439–5449.

Homma, M., Fujita, H., Yamaguchi, S. & Iino, T. 1984 Excretion of unassembled flagellin by *Salmonella typhimurium* mutants deficient in hook-associated proteins. *J. Bacteriol.* **159**, 1056–1059.

Homma, M., Komeda, Y., Iino, T. & Macnab, R. M. 1987 The *flaFIX* gene product of *Salmonella typhimurium* is a flagellar basal body component with a signal peptide for export. *J. Bacteriol.* **169**, 1493–1498.

Iino, T. 1969 Polarity of flagellar growth in *Salmonella*. *J. Gen. Microbiol.* **56**, 227–239.

Iino, T. 1974 Assembly of *Salmonella* flagellin *in vitro* and *in vivo*. *J. Supramol. Struct.* **2**, 372–384.

Iino, T., Komeda, Y., Kutsukake, K., Macnab, R. M., Matsumura, P., Parkinson, J. S., Simon, M. I. & Yamaguchi, S. 1988 New unified nomenclature for the flagellar genes of *Escherichia coli* and *Salmonella typhimurium*. *Microbiol. Rev.* **52**, 533–535.

Ikeda, T., Homma, M., Iino, T., Asakura, S. & Kamiya, R. 1987 Localization and stoichiometry of hook-associated proteins within *Salmonella typhimurium* flagella. *J. Bacteriol.* **169**, 1168–1173.

Ikeda, T., Yamaguchi, S. & Hotani, H. 1993 Flagellar growth in a filament-less *Salmonella fliD* mutant supplemented with purified hook-associated protein 2. *J. Biochem.* **114**, 39–44.

Ikeda, T., Oosawa, K. & Hotani, H. 1996 Self-assembly of the filament capping protein, FliD, of bacterial flagella into an annular structure. *J. Mol. Biol.* **259**, 679–686.

Imae, Y. 1991 Use of Na^+ as an alternative to H^+ in energy transduction. In *New era of bioenergetics* (ed. Y. Mukohata), pp. 197–221. Tokyo: Academic Press.

Imae, Y. & Atsumi, T. 1989 Na^+-driven bacterial flagellar motors. *J. Bioenerg. Biomembr.* **21**, 705–716.

Iwazawa, J., Imae, Y. & Kobayasi, S. 1993 Study of the torque of the bacterial flagellar motor using a rotating electric field. *Biophys. J.* **64**, 925–933.

Jeffery, G. B. 1915 On the steady rotation of a solid of revolution in a viscous fluid. *Proc. Lond. Math. Soc.* **14**, 327–338.

PHILOSOPHICAL TRANSACTIONS OF THE ROYAL SOCIETY B BIOLOGICAL SCIENCES

Jones, C. J., Homma, M. & Macnab, R. M. 1989 L-, P-, and M-ring proteins of the flagellar basal body of *Salmonella typhimurium*: gene sequences and deduced protein sequences. *J. Bacteriol.* **171**, 3890–3900.

Kagawa, H., Morisawa, H. & Enomoto, M. 1981 Reconstitution *in vitro* of flagellar filaments onto hook structures attached to bacterial cells. *J. Mol. Biol.* **153**, 465–470.

Kagawa, H., Nishiyama, T. & Yamaguchi, S. 1983 Motility development of *Salmonella typhimurium* cells with *flaV* mutations after addition of exogenous flagellin. *J. Bacteriol.* **155**, 435–437.

Kami-ike, N., Kudo, S. & Hotani, H. 1991 Rapid changes in flagellar rotation induced by external electric pulses. *Biophys. J.* **60**, 1350–1355.

Kara-Ivanov, M., Eisenbach, M. & Caplan, S. R. 1995 Fluctuations in rotation rate of the flagellar motor of *Escherichia coli*. *Biophys. J.* **69**, 250–263.

Kashket, E. R. 1985 The proton motive force in bacteria: a critical assessment of methods. *A. Rev. Microbiol.* **39**, 219–242.

Khan, I. H., Reese, T. S. & Khan, S. 1992 The cytoplasmic component of the bacterial flagellar motor. *Proc. Natl Acad. Sci. USA* **89**, 5956–5960.

Khan, S. & Berg, H. C. 1983 Isotope and thermal effects in chemiosmotic coupling to the flagellar motor of *Streptococcus*. *Cell* **32**, 913–919.

Khan, S. & Macnab, R. M. 1980*a* Proton chemical potential, proton electrical potential and bacterial motility. *J. Mol. Biol.* **138**, 599–614.

Khan, S. & Macnab, R. M. 1980*b* The steady-state counterclockwise/clockwise ratio of bacterial flagellar motors is regulated by protonmotive force. *J. Mol. Biol.* **138**, 563–597.

Khan, S., Meister, M. & Berg, H. C. 1985 Constraints on flagellar rotation. *J. Mol. Biol.* **184**, 645–656.

Khan, S., Dapice, M. & Reese, T. S. 1988 Effects of mot gene expression on the structure of the flagellar motor. *J. Mol. Biol.* **202**, 575–584.

Khan, S., Dapice, M. & Humayun, I. 1990 Energy transduction in the bacterial flagellar motor: effects of load and pH. *Biophys. J.* **57**, 779–796.

Khan, S., Khan, I. H. & Reese, T. S. 1991 New structural features of the flagellar base in *Salmonella typhimurium* revealed by rapid-freeze electron microscopy. *J. Bacteriol.* **173**, 2888–2896.

Khan, S., Ivey, D. M. & Krulwich, T. A. 1992 Membrane ultrastructure of alkaliphilic *Bacillus* species studied by rapid-freeze electron microscopy. *J. Bacteriol.* **174**, 5123–5126.

Kihara, M., Francis, N. R., DeRosier, D. J. & Macnab, R. M. 1996 Analysis of a FliM-FliN flagellar switch fusion mutant of *Salmonella typhimurium*. *J. Bacteriol.* **178**, 4582–4589.

Kojima, S., Atsumi, T., Muramoto, K., Kudo, S., Kawagishi, I. & Homma, M. 1997 *Vibrio alginolyticus* mutants resistant to phenamil, a specific inhibitor of the sodium-driven flagellar motor. *J. Mol. Biol.* **265**, 310–318.

Kojima, S., Asai, Y., Atsumi, T., Kawagishi, I. & Homma, M. 1999 Na^+-driven flagellar motor resistant to phenamil, an amiloride analogue, caused by mutations in putative channel components. *J. Mol. Biol.* **285**, 1537–1547.

Kubori, T., Shimamoto, N., Yamaguchi, S., Namba, K. & Aizawa, S.-I. 1992 Morphological pathway of flagellar assembly in *Salmonella typhimurium*. *J. Mol. Biol.* **226**, 433–446.

Kubori, T., Yamaguchi, S. & Aizawa, S.-I. 1997 Assembly of the switch complex onto the MS ring complex of *Salmonella typhimurium* does not require any other flagellar proteins. *J. Bacteriol.* **179**, 813–817.

Kutsukake, K., Minamino, T. & Yokoseki, T. 1994 Isolation and characterization of FliK-independent flagellation mutants from *Salmonella typhimurium*. *J. Bacteriol.* **176**, 7625–7629.

Larsen, S. H., Adler, J., Gargus, J. J. & Hogg, R. W. 1974 Chemomechanical coupling without ATP: the source of energy for motility and chemotaxis in bacteria. *Proc. Natl Acad. Sci. USA* **71**, 1239–1243.

Läuger, P. 1988 Torque and rotation rate of the bacterial flagellar motor. *Biophys. J.* **53**, 53–65.

Läuger, P. & Kleutsch, B. 1990 Microscopic models of the bacterial flagellar motor. *Comments Theor. Biol.* **2**, 99–123.

Lloyd, S. A. & Blair, D. F. 1997 Charged residues of the rotor protein FliG essential for torque generation in the flagellar motor of *Escherichia coli*. *J. Mol. Biol.* **266**, 733–744.

Lloyd, S. A., Tang, H., Wang, X., Billings, S. & Blair, D. F. 1996 Torque generation in the flagellar motor of *Escherichia coli*: evidence of a direct role for FliG but not for FliM or FliN. *J. Bacteriol.* **178**, 223–231.

Lowe, G., Meister, M. & Berg, H. C. 1987 Rapid rotation of flagellar bundles in swimming bacteria. *Nature* **325**, 637–640.

Ludwig, W. 1930 Zur Theorie der Flimmerbewegung (Dynamik, Nutzeffekt, Energiebalanz). *Z Vgl. Physiol.* **13**, 397–504.

Macnab, R. M. 1995 Flagellar switch. In *Two-component signal transduction* (ed. J. A. Hoch & T. J. Silhavy), pp. 181–199. Washington, DC: American Society for Microbiology.

Magariyama, Y., Sugiyama, S., Muramoto, K., Maekawa, Y., Kawagishi, I., Imae, Y. & Kudo, S. 1994 Very fast flagellar rotation. *Nature* **371**, 752.

Malakooti, J., Ely, B. & Matsumura, P. 1994 Molecular characterization, nucleotide sequence, and expression of the *fliO*, *fliP*, *fliQ*, and *fliR* genes of *Escherichia coli*. *J. Bacteriol.* **176**, 189–197.

Manson, M. D., Tedesco, P., Berg, H. C., Harold, F. M. & Van der Drift, C. 1977 A protonmotive force drives bacterial flagella. *Proc. Natl Acad. Sci. USA* **74**, 3060–3064.

Manson, M. D., Tedesco, P. M. & Berg, H. C. 1980 Energetics of flagellar rotation in bacteria. *J. Mol. Biol.* **138**, 541–561.

Matsuura, S., Shioi, J.-I. & Imae, Y. 1977 Motility in *Bacillus subtilis* driven by an artificial protonmotive force. *FEBS Lett.* **82**, 187–190.

Matsuura, S., Shioi, J.-I., Imae, Y. & Iida, S. 1979 Characterization of the *Bacillus subtilis* motile system driven by an artificially created proton motive force. *J. Bacteriol.* **140**, 28–36.

Meister, M. & Berg, H. C. 1987 The stall torque of the bacterial flagellar motor. *Biophys. J.* **52**, 413–419.

Meister, M., Lowe, G. & Berg, H. C. 1987 The proton flux through the bacterial flagellar motor. *Cell* **49**, 643–650.

Meister, M., Caplan, S. R. & Berg, H. C. 1989 Dynamics of a tightly coupled mechanism for flagellar rotation. *Biophys. J.* **55**, 905–914.

Mitchell, P. 1956 Hypothetical thermokinetic and electrokinetic mechanisms of locomotion in micro-organisms. *Proc. R. Phys. Soc. Edinb.* **25**, 32–34.

Mitchell, P. 1972 Self-electrophoretic locomotion in micro-organisms: bacterial flagella as giant ionophores. *FEBS Lett.* **28**, 1–4.

Muramoto, K., Kawagishi, I., Kudo, S., Magariyama, Y., Imae, Y. & Homma, M. 1995 High-speed rotation and speed stability of the sodium-driven flagellar motor in *Vibrio alginolyticus*. *J. Mol. Biol.* **251**, 50–58.

Ohnishi, K., Ohto, Y., Aizawa, S.-I., Macnab, R. M. & Iino, T. 1994 FlgD is a scaffolding protein needed for flagellar hook assembly in *Salmonella typhimurium*. *J. Bacteriol.* **176**, 2272–2281.

Ohnishi, K., Fan, F., Schoenhals, G. J., Kihara, M. & Macnab, R. M. 1997 The FliO, FliP, FliQ, and FliR proteins of *Salmonella typhimurium*: putative components for flagellar assembly. *J. Bacteriol.* **179**, 6092–6099.

Okino, H., Isomura, M., Yamaguchi, S., Magariyama, Y., Kudo, S. & Aizawa, S.-I. 1989 Release of flagellar filament-hook–rod

complex by a *Salmonella typhimurium* mutant defective in the M ring of the basal body. *J. Bacteriol.* **171**, 2075–2082.
Purcell, E. M. 1977 Life at low Reynolds number. *Am. J. Phys.* **45**, 3–11.
Ravid, S. & Eisenbach, M. 1984 Minimal requirements for rotation of bacterial flagella. *J. Bacteriol.* **158**, 1208–1210.
Ridgway, H. F., Silverman, M. & Simon, M. I. 1977 Localization of proteins controlling motility and chemotaxis in *Escherichia coli*. *J. Bacteriol.* **132**, 657–665.
Samuel, A. D. T. & Berg, H. C. 1995 Fluctuation analysis of rotational speeds of the bacterial flagellar motor. *Proc. Natl Acad. Sci. USA* **92**, 3502–3506.
Samuel, A. D. T. & Berg, H. C. 1996 Torque-generating units of the bacterial flagellar motor step independently. *Biophys. J.* **71**, 918–923.
Schoenhals, G. J. & Macnab, R. M. 1996 Physiological and biochemical analyses of FlgH, a lipoprotein forming the outer membrane L ring of the flagellar basal body of *Salmonella typhimurium*. *J. Bacteriol.* **178**, 4200–4207.
Sharp, L. L., Zhou, J. & Blair, D. F. 1995*a* Features of MotA proton channel structure revealed by tryptophan-scanning mutagenesis. *Proc. Natl Acad. Sci. USA* **92**, 7946–7950.
Sharp, L. L., Zhou, J. & Blair, D. F. 1995*b* Tryptophan-scanning mutagnesis of Mot B, an integral membrane protein essential for flagellar rotation in *Escherichia coli*. *Biochemistry* **34**, 9166–9171.
Shioi, J.-I., Matsuura, S. & Imae, Y. 1980 Quantitative measurements of protonmotive force and motility in *Bacillus subtilis*. *J. Bacteriol.* **144**, 891–897.
Silverman, M. & Simon, M. 1974 Flagellar rotation and the mechanism of bacterial motility. *Nature* **249**, 73–74.
Skulachev, V. P. 1975 Electric generators in coupling membranes: direct measurements of the electrogenic activity, molecular mechanisms and some specific functions. In *Enzymes, electron transport systems; proceedings of the tenth FEBS meeting*, vol. 40 (ed. P. Desnuelle & A. M. Michelson), pp. 225–238. Amsterdam: North-Holland.
Stader, J., Matsumura, P., Vacante, D., Dean, G. E. & Macnab, R. M. 1986 Nucleotide sequence of the *Escherichia coli motB* gene and site-limited incorporation of its product into the cytoplasmic membrane. *J. Bacteriol.* **166**, 244–252.
Sugiyama, S., Cragoe Jr, E. J. & Imae, Y. 1988 Amiloride, a specific inhibitor for the Na^+-driven flagellar motors of alkalophilic *Bacillus*. *J. Biol. Chem.* **263**, 8215–8219.
Suzuki, T. & Komeda, Y. 1981 Incomplete flagellar structures in *Escherichia coli* mutants. *J. Bacteriol.* **145**, 1036–1041.
Suzuki, T., Iino, T., Horiguchi, T. & Yamaguchi, S. 1978 Incomplete flagellar structures in nonflagellate mutants of *Salmonella typhimurium*. *J. Bacteriol.* **133**, 904–915.
Svoboda, K., Mitra, P. P. & Block, S. M. 1994 Fluctuation analysis of motor protein movement and single enzyme kinetics. *Proc. Natl Acad. Sci. USA* **91**, 11 782–11 786.
Tang, H., Braun, T. F. & Blair, D. F. 1996 Motility protein complexes in the bacterial flagellar motor. *J. Mol. Biol.* **261**, 209–221.
Taylor, G. I. 1952 The action of waving cylindrical tails in propelling microscopic organisms. *Proc. R. Soc. Lond* A **211**, 225–239.
Ueno, T., Oosawa, K. & Aizawa, S.-I. 1992 M ring, S ring and proximal rod of the flagellar basal body of *Salmonella typhimurium* are composed of subunits of a single protein, FliF. *J. Mol. Biol.* **227**, 672–677.
Ueno, T., Oosawa, K. & Aizawa, S.-I. 1994 Domain structures of the MS ring component protein (FliF) of the flagellar basal body of *Salmonella typhimurium*. *J. Mol. Biol.* **236**, 546–555.
Van der Drift, C., Duiverman, J., Bexkens, H. & Krijnen, A. 1975 Chemotaxis of a motile *Streptococcus* toward sugars and amino acids. *J. Bacteriol.* **124**, 1142–1147.
Vogler, A. P., Homma, M., Irikura, V. M. & Macnab, R. M. 1991 *Salmonella typhimurium* mutants defective in flagellar filament regrowth and sequence similarity of FliI to F_0F_1, vacuolar, and archaebacterial ATPase subunits. *J. Bacteriol.* **173**, 3564–3572.
Washizu, M., Kurahashi, Y., Iochi, H., Kurosawa, O., Aizawa, S.-I., Kudo, S., Magariyama, Y. & Hotani, H. 1993 Dielectrophoretic measurement of bacterial motor characteristics. *IEEE Trans. Ind. Applicat.* **29**, 286–294.
Yamaguchi, S., Aizawa, S.-I., Kihara, M., Isomura, M., Jones, C. J. & Macnab, R. M. 1986*a* Genetic evidence for a switching and energy-transducing complex in the flagellar motor of *Salmonella typhimurium*. *J. Bacteriol.* **168**, 1172–1179.
Yamaguchi, S., Fujita, H., Ishihara, A., Aizawa, S.-I. & Macnab, R. M. 1986*b* Subdivision of flagellar genes of *Salmonella typhimurium* into regions responsible for assembly, rotation, and switching. *J. Bacteriol.* **166**, 187–193.
Zhao, R., Schuster, S. C. & Khan, S. 1995 Structural effects of mutations in *Salmonella typhimurium* flagellar switch complex. *J. Mol. Biol.* **251**, 400–412.
Zhao, R., Pathak, N., Jaffe, H., Reese, T. S. & Khan, S. 1996 FliN is a major structural protein of the C-ring in the *Salmonella typhimurium* flagellar basal body. *J. Mol. Biol.* **261**, 195–208.
Zhou, J. & Blair, D. F. 1997 Residues of the cytoplasmic domain of MotA essential for torque generation in the bacterial flagellar motor. *J. Mol. Biol.* **273**, 428–439.
Zhou, J., Fazzio, R. T. & Blair, D. F. 1995 Membrane topology of the MotA protein of *Escherichia coli*. *J. Mol. Biol.* **251**, 237–242.
Zhou, J., Lloyd, S. A. & Blair, D. F. 1998*a* Electrostatic interactions between rotor and stator in the bacterial flagellar motor. *Proc. Natl Acad. Sci. USA* **95**, 6436–6441.
Zhou, J., Sharp, L. L., Tang, H. L., Lloyd, S. A., Billings, S., Braun, T. F. & Blair, D. F. 1998*b* Function of protonatable residues in the flagellar motor of *Escherichia coli*: a critical role for Asp 32 of MotB. *J. Bacteriol.* **180**, 2729–2735.

PHILOSOPHICAL TRANSACTIONS OF THE ROYAL SOCIETY B BIOLOGICAL SCIENCES

PHILOSOPHICAL TRANSACTIONS OF THE ROYAL SOCIETY B BIOLOGICAL SCIENCES